tvst

Article

Field Expansion with Multiplexing Prism Glasses Improves Pedestrian Detection for Acquired Monocular Vision

Jae-Hyun Jung[1], Rachel Castle[1], Nish Mohith Kurukuti[1], Sailaja Manda[1], and Eli Peli[1]

[1] Schepens Eye Research Institute of Massachusetts Eye and Ear, Department of Ophthalmology, Harvard Medical School, Boston, MA, USA

Correspondence: Jae-Hyun Jung, PhD, FAAO, Schepens Eye Research Institute, 20 Staniford St, Boston, MA 02114, USA. e-mail: jaehyun_jung@meei.harvard.edu

Received: February 5, 2020
Accepted: April 23, 2020
Published: July 23, 2020

Keywords: field expansion; vision multiplexing; monocular vision; prism; collision; 3D printing; simulator

Citation: Jung J-H, Castle R, Kurukuti NM, Manda S, Peli E. Field expansion with multiplexing prism glasses improves pedestrian detection for acquired monocular vision. Trans Vis Sci Tech. 2020;9(8):35, https://doi.org/10.1167/tvst.9.8.35

Purpose: Patients with acquired monocular vision (AMV) lose vision in the temporal crescent on the side of the blind eye. This visual field loss affects patients' ability to detect potential hazards in the blind field. Mounting a base-in multiplexing prism (MxP) on the nasal side of the seeing eye can provide true field expansion and enable detection of potential collision hazards. We evaluated the efficacy of the MxP glasses in a virtual reality walking environment.

Methods: A three-dimensional printed clip-on MxP holder that can be adjusted for an individual user's facial parameters was developed. Virtual reality walking scenarios were designed to evaluate the effect of MxP field expansion on the detection of a pedestrian approaching from different initial bearing angles and courses. The pedestrian detection rates and response times of 10 participants with simulated AMV (normally sighted participants with one eye patched) and three patients with AMV were measured.

Results: The MxP provided true field expansion of about 25°. Participants performed significantly better with the MxP than without the MxP in the pedestrian detection task on their blind field, while their seeing field performance was not significantly different.

Conclusions: The MxP glasses for patients with AMV improved the detection of potential collision hazards in the blind field.

Translational Relevance: The MxP with an adjustable clip-on holder may help patients with AMV to decrease the risk of collision with other pedestrians.

Introduction

Acquired monocular vision (AMV),[1,2] the loss of sight in one eye, can occur from injury or ocular disease. Brady[3] reported that approximately 50,000 people lose an eye each year in the United States, mostly due to injury. Another population-based study estimated the annual incidence of enucleation secondary to trauma and disease to be 4.3 per 100,000 people.[4] AMV results in loss of binocular stereo vision and a decreased visual field, as well as the social and psychological impact of the loss.[1] At least two-thirds of patients with AMV reported difficulties with distance judgments and peripheral vision tasks.[5] After a period of adaptation, patients with AMV learn to rely on monocular depth cues to compensate for the loss of stereo vision, but the visual field loss is permanent.[6]

The normal horizontal binocular visual field is about 200°.[7,8] A single eye can monitor up to 105° temporally from the vertical midline but only approximately 55° nasally.[8] Note that the blind field in this paper means the temporal crescent on the side of the blind eye (nasal side of the seeing eye).

Patients with AMV often report collisions with pedestrians approaching from the blind field.[1,6] Peli et al.[9] analyzed the risk of pedestrian collisions in open environments, such as shopping malls or transportation terminals, as a function of pedestrian bearing angle (the relative angle of a pedestrian from the patients' heading). When a patient and a pedestrian are walking straight on a collision course with a constant speed, the pedestrian remains at a fixed bearing angle. A colliding pedestrian who first appears in blind field will never enter the seeing field and thus is difficult to avoid, unless the patient scans into

the blind field.[9,10] Based on the risk density graph in Figure 4 of Peli et al.,[9] patients with AMV would miss approximately 15% of the collision risk (area under the graph that corresponds with the missing temporal crescent[9]). Even though patients with AMV can monitor the blind field with frequent head scans, they may not really know when a scan is needed.

Various devices have been proposed and developed in attempts to expand the visual field of patients with AMV.[1,11,12] However, these devices provide field substitution (no change in the total size of the field of view) at best but no true field expansion.[13,14]

We recently analyzed the use of a high power, 57 prism diopter (Δ), base-in Fresnel prism segment placed over the nose bridge on the seeing eye for patients with AMV to shift a portion of the unseen field into the seeing field,[13] but the shifted view through the Fresnel prism would only replace a portion of the seeing field due to the apical scotoma (Fig. 1 of Apfelbaum et al.).[15] To eliminate the apical scotoma and achieve true field expansion with one eye, a new optical element, the multiplexing prism (MxP),[16] can be used to provide a shifted view superimposed with a see-through (unshifted) view.

To eliminate the total internal reflection caused by the high angle of incidence,[17] we proposed fitting the MxP with the serrations facing toward the eye (eyeward prism serration)[17] with a negative face-form tilt.[13] The tilt angle and width of MxP would need to be individually fitted based on pupillary distance, back vertex distance, refractive correction, and nasal extent of the visual field. The early prototypes[13] provided true field expansion for patients with AMV with a horizontal extent of up to 195°, close to the extent of the normal binocular visual field. However, the fixtures used were not easily adjustable for individual patients and thus would be impractical in clinical settings. In this paper, we designed and tested a three-dimensional (3D) printed clip-on holder to easily adjust the tilt of MxP segment for individual patients. The 3D printing technology facilitated design flexibility, cost effectiveness ($2 per holder), and a fast turnaround time for prototyping in this study.

The MxP achieves true field expansion through monocular visual confusion of the shifted and see-through views. The superimposed views have reduced the contrast of each other[16] and different motions, which may affect the detection performance in either view. Although the prototype MxP glasses were measured by perimetry,[13] an outcome measure in a more realistic setting is needed to evaluate the efficacy of the MxP glasses. Perimetry has only a single bright target on a blank background, and thus no visual confusion (no conflicting motion) occurs between the two views, and the effect of reduced contrast is small. Additionally, when a patient is walking and looking straight ahead, a colliding pedestrian appears at a fixed bearing angle (fixed retinal eccentricity), the angular size increases (looming) with moving background.[9,10] In (kinetic) perimetry, we measure the detection of a moving target (on a blank background) without looming.

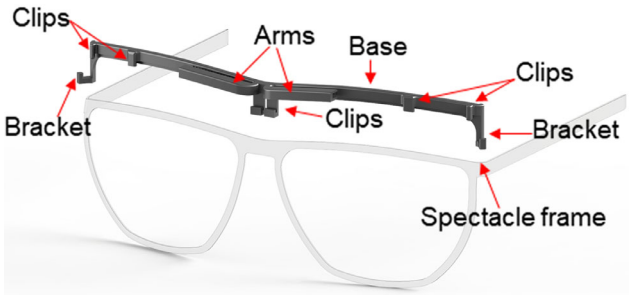

Figure 1. Design of the 3D-printed clip-on MxP holder. The holder is designed to fit the top rim of the spectacles frame and is mounted using clips and brackets. The MxP segment is attached to one of the two arms depending on the side of vision loss.

To evaluate the efficacy of MxP in AMV for pedestrian detection and collision judgment, we modified our driving simulator and developed virtual reality (VR) walking scenarios.[18] Participants were seated in the simulator while the screen presented moving scenes to simulate the participants' walking. In the VR walking scenarios, participants moved at a simulated brisk walking speed on a predetermined path as other pedestrians appeared and walked toward the participant's path. With pedestrians appearing in the see-through or shifted view, the impact of monocular visual confusion on the pedestrian detection was evaluated.

Methods

3D-Printed Clip-on MxP Holder Design

We designed a 3D-printed clip-on MxP holder to be mounted on a spectacles frame (Fig. 1). The clip-on MxP holder has two arms that give the holder a symmetric look and allow us to mount the MxP segment on either side of the spectacle lens for right or left AMV. The arm holds the MxP segment in front of the spectacles lens to incorporate the refractive correction. The MxP segment has two small hooks at the top, which fit into two matching slots in the arms (Fig. 2).

To adjust the tilt angle of the MxP segment, we designed a mechanism that rotates the flexible arm (holding the MxP) through elastic body deformation (Fig. 3). Grooves in the arm and base of the holder are

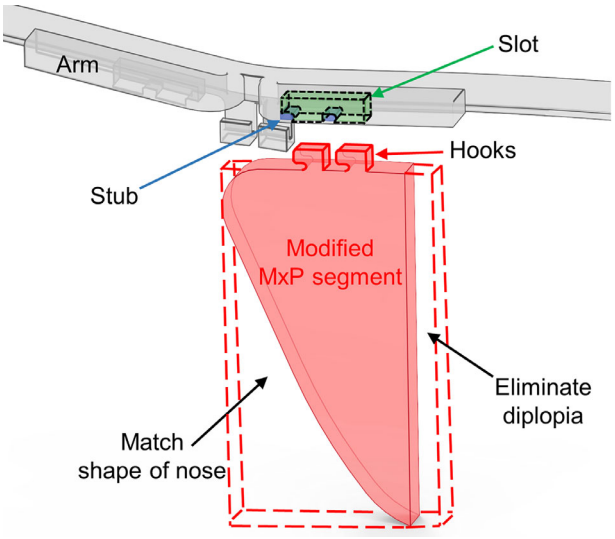

Figure 2. Mounting MxP segment. Hooks (solid red) on the MxP segment are inserted in the slots (green area) in the arm. The hooks rest on the blue stubs in the slot. The MxP segment is produced in a rectangular shape (dashed red) and then trimmed to accommodate the nose on one side and to eliminate possible diplopia on the other.[13]

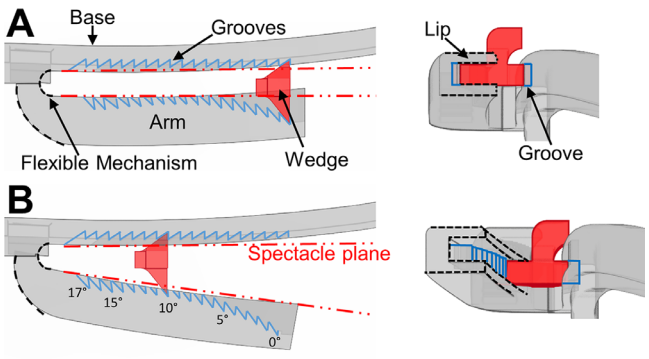

Figure 3. Top view (left) and side view (right) of the flexible mechanism used to adjust the tilt angle of the MxP. (A) A moveable wedge is placed in the grooves between the body and arm. The grooves have lips on the top and bottom, restricting the wedge from popping out of the grooves. (B) Each successive step of the wedge in the grooves rotates the arm (MxP) by 1° with respect to the spectacles frame within the range of 0° to 17°. The wedge is glued in place after the fitting.

designed to hold a corresponding moveable wedge that rotates the arm with respect to the spectacles frame.

Polyamide 11 (Nylon 11) was selected to 3D print the clip-on holder to obtain required flexibility, using selective laser sintering technology.[19] Thin and lightweight frames with narrow nose bridge (55-15-140, Michelle Moretti 206, GlassesUSA.com) were selected to minimize field blocking by the frame.[20,21]

The MxP segments were produced by shaving the tops of conventional polymethyl methacrylate (PMMA) Fresnel prisms and then machined to produce the hooks (Chadwick Optical, Harleysville, PA).[16] The MxP segment was mounted using the hook mechanism after the nasal side of the segment was trimmed to accommodate the nose of the individual patient.[13]

Participants

Ten normally sighted participants (4 women) were recruited to participate as simulated AMV. The average age was 27.8 ± 4.5 years. All had corrected binocular visual acuity (with contact lens if needed) of 20/32 or better and a horizontal binocular visual field of at least 180° (Goldmann Perimeter with the V4e stimulus). AMV was simulated using an adhesive eye patch over the right or left eye, alternated by the recruitment order.

Three patients with AMV were recruited (21, 41, and 70 years old; 1 woman). Two patients had a visual acuity of 20/25 in the seeing eye, and the third had a visual acuity of 20/40. All patients had little to no light perception in the blind eye.

All study procedures were approved by the Massachusetts Eye and Ear Human Studies Committee and carried out in accordance with the tenets of the Declaration of Helsinki. Written and informed consent was obtained from all participants before the beginning of the procedures.

Fitting Procedures

The nasal extent of the monocular visual field (Goldmann Perimeter with the V4e stimulus, Haag-Streit, Berne, Germany), pupillary distance (PM-200 pupilometer, LuxVision, US Ophthalmic, Doral, FL), and back vertex distance (Distometer, Western Ophthalmics, Lynnewood, WA) were measured. We calculated the required tilt angle of the MxP from individual parameters.[13]

For simulated AMV, we prepared only two pairs of spectacles with the clip-on MxP holder for all participants (one for left AMV and the other for right AMV) and adjusted only the tilt angle for each participant (Fig. 4). The width of the MxP segments (17 mm) remained constant for all simulated AMV participants. This value was calculated by assuming a pupillary distance of 32.5 mm, distance between the back vertex of the lens and the entrance pupil of 16 mm, and a nasal field extent of 55°.[13] The 17-mm MxP segment would cover the seeing nasal field from 37° (the apex) to the end of the nasal field (base). The field expansion provided by the customized MxP glasses was measured in the Goldmann perimeter. We iteratively adjusted the

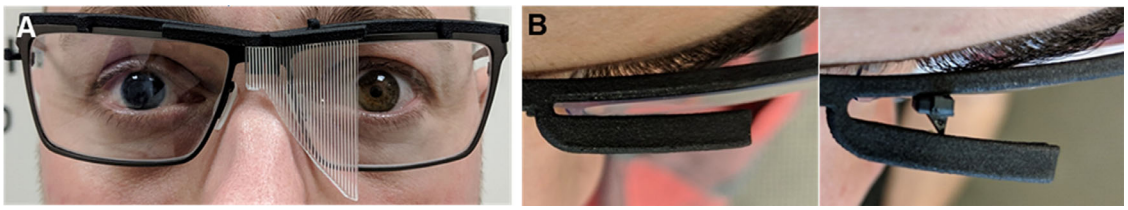

Figure 4. Spectacles with the 3D printed clip-on MxP holder fit on a participant with left AMV. (A) The MxP segment is trimmed to match the contour of the nose of the individual. The MxP extends over the nose bridge to allow the scanning of the seeing eye (left eye here) toward the blind field (toward the blind eye) outside the frame. (B) The wedge is placed in the grooves to rotate the arm to the required negative face-form tilt angle.

tilt angle (Fig. 4B) and repeated the perimetry to determine the optimal tilt angle that provided maximum field expansion.

For patients with AMV, we measured individual parameters, including the spectacles lens prescription. The MxP segment was first positioned at the calculated tilt angle based on the patient's parameters[13] and then the tilt angle was iteratively adjusted to achieve maximum field expansion as measured by perimetry. The MxP segment was then trimmed to the required width to minimize both diplopia and scotoma at the primary position of gaze with repeated perimetry (Supplementary Material, Appendix A).[13] After maximum field expansion was achieved, the wedge was glued to the clip-on holder.

Walking Simulator Scenarios

A driving simulator with a 225° field of view provided by the 5 LCD monitors (LE1500; FAAC INC, Ann Arbor, MI) was used to simulate walking in an open park (Fig. 5). A bicycle model instead of a car was used to provide a full view of the simulator environment (i.e., avoiding blocking from pillars of the car). Participants were seated 74 cm from the front screen.[18] The simulated walking speed was set at a constant 1.4 m/s (3.1 miles/hour) to simulate a brisk walking speed in a city,[22] and the gas and brake pedals were not used.

The participants followed a predefined walking course through an open field VR environment with buildings, roads, and vehicles visible in the background. To ensure participants stayed on the designated path, they were instructed to follow an orange basketball by keeping it aligned with a string at the center of the front screen using the steering wheel. This task kept the participant attending to the path.

While the participant followed the basketball, pedestrians appeared on the left or right at an initial bearing of 45°, 65°, or 80° and walked toward the participant's path. The bearing angle is the angle of the pedestrian relative to the patient's heading. When a participant is looking straight, the bearing angle of the pedestrian is the same as visual eccentricity.

Three pedestrian course types were simulated: center-to-center collision, near-collision, and non-collision. The pedestrians would cross the participant's path 6 seconds after the initial appearance, though all pedestrians disappeared 0.1 seconds before reaching the participant's path so that no visible collisions occurred. To keep 6 seconds of walking time with different courses and initial bearing angle, the pedestrian's walking speed was different among courses but was constant within each course. Different courses are described by the path crossing distance (d_{pc}), the participant's distance from the point where the pedestrian would cross the participant.[18]

On a center-to-center collision (d_{pc}, $d_{pc} = 0$), the pedestrian initially appears at one of the bearing angles and remains at that initial bearing until disappearing just before the collision (Fig. 6; see Supplementary Material, Appendix B1 for details of movies, and see Supplementary Movies B1A, B1B, and B1C). If the colliding pedestrian appears in the blind field, the pedestrian is not detectable unless the participant turns the head toward the blind field. Eye scanning alone will not bring the pedestrian into the seeing field because the view will be blocked by the nose.[13,14] Patients with AMV do not know when the pedestrian appears in the blind field and thus do not know when to scan.

Participants may judge pedestrians who pass in front of or behind the participant as a collision even though they are not on the center-to-center collision course. In our preliminary study with the VR walking scenario in the same environment (IOVS. 2017;58:ARVO E-Abstract 3287), a 30° initial bearing pedestrian passing within 2 m in front of ($d_{pc} = +2$ m) or behind ($d_{pc} = -2$ m) were judged by normally sighted participants as a collision. Given this result, we categorized pedestrians who crossed 2 m in front of (Fig. 7A) or behind the participant (Fig. 7B) as a near-collision. Non-collision course pedestrians crossed much farther ($d_{pc} = 12$ m) in front of the participant (Fig. 7C). The bearing angles of the near-collision and noncollision

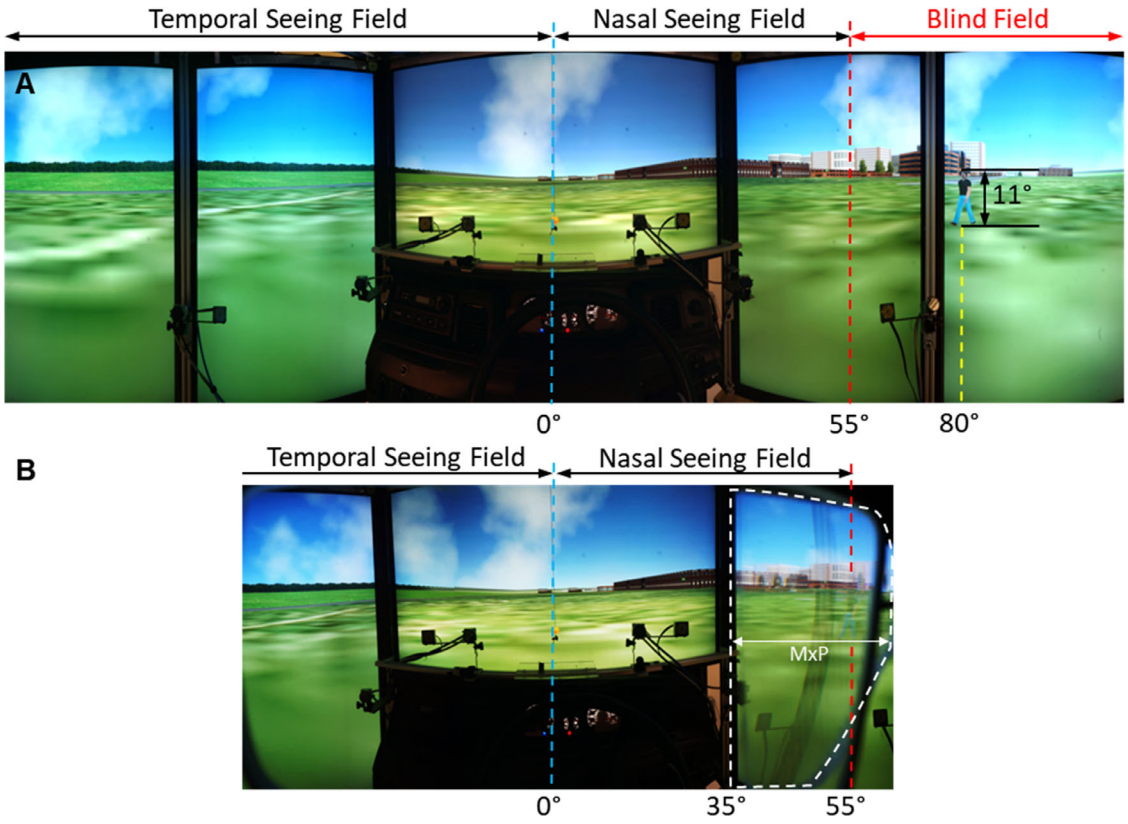

Figure 5. VR walking scenario in the driving simulator. The blue dashed line at 0° marks the center of the front monitor. (A) Panoramic view of the walking scenario as seen from a participant with normal vision as a pedestrian approaches the participant on the right at 80° bearing. (B) Panoramic view with 3D printed clip-on MxP holder for a patient with left AMV. The MxP (white dashed line) shows the same pedestrian in the shifted view as the field expansion, superimposed over the see-through view of the buildings at 55°. Note the prism distortion of the right display bezel in the shifted view through the MxP.

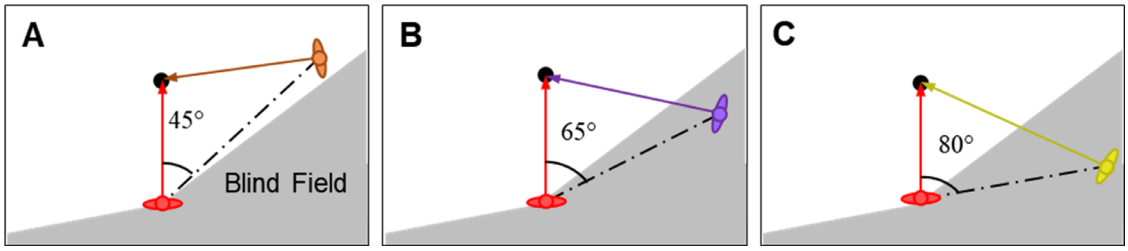

Figure 6. Pedestrians on center-to-center collision courses with left AMV. The gray area marks the blind field of a patient with left AMV. (A) A 45° bearing pedestrian (see Supplementary Movie B1A), (B) a 65° bearing pedestrian (see Supplementary Movie B1B), and (C) an 80° bearing pedestrian (see Supplementary Movie B1C). The solid black circle represents the collision point. These colliding pedestrians would stay at a fixed bearing angle with respect to the participant (red) for the entire event. The 65° and 80° bearing pedestrians would stay in the blind field and are not detectable by patients with AMV without scanning into the blind field. See Supplementary Material, Appendix B1 for details of movies.

course pedestrians are not constant. Pedestrians that cross in front of the participant move toward the central field from the initial bearing, whereas pedestrians that cross behind move farther into the periphery (see Supplementary Material, Appendix B2 for details of movies, and see Supplementary Movies B2A, B2B, and B2C).

Pedestrian Detection Study

After fitting the MxP glasses, participants completed an introductory scenario to become familiar with the VR walking environment and tasks. This introductory scenario took approximately 10 minutes and included the same task but a different order of

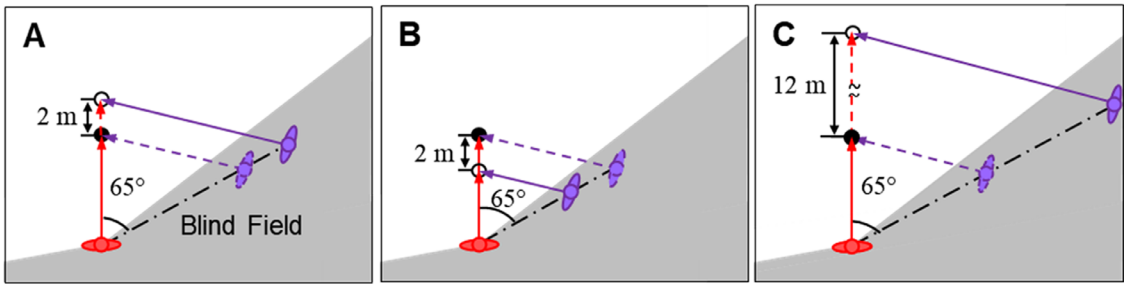

Figure 7. Pedestrians (initially appear at 65° as an example) on (A and B) near-collision and (C) noncollision courses defined by path crossing distance (d_{pc}). The solid red line marks the participant's path, and the solid black circle represents the participant's location after walking for six seconds. A pedestrian who crosses (A) 2 m in front of ($d_{pc} = +2$ m) (see Supplementary Movie B2A) or (B) 2 m behind ($d_{pc} = -2$ m) (see Supplementary Movie B2B) the collision point is defined as a near-collision. (C) A noncollision course pedestrian crosses 12 m in front of the participant ($d_{pc} = +12$ m) (see Supplementary Movie B2C). The violet line and the open circle mark the pedestrian's path and locations after six seconds (solid line for the actual course and dashed line for center-to-center collision course). See Supplementary Material, Appendix B2 for details of movies.

pedestrian events than those included in the study. Once they demonstrated a clear understanding of the tasks, they began the scored scenarios.

Normal vision participants were tested under three viewing conditions: normal (binocular) vision (NV), simulated AMV (AMV), and simulated AMV with MxP for field expansion (AMV+MxP). Patients with AMV were tested with and without the MxP (AMV+MxP and AMV, respectively). The scenario and viewing condition orders were randomized for each subject.

Participants completed a total of six scenarios. Each scenario was divided into 24 segments with one pedestrian encounter per segment. At the beginning of each segment, the basketball changed direction slightly ($\leq 5°$) to engage the participants in the task, after which participants were given at least 9 seconds to realign the ball to the string before a pedestrian might appear. Each scenario lasted approximately 10 minutes. The 24 pedestrian events included 4 at each of the 3 eccentricities on the right and left with path crossing distance (d_{pc}) of –2 m, 0 m, +2 m, and +12 m, such that each pedestrian encounter was different from all others in a single scenario. The order of eccentricity and path crossing distance was randomized to minimize any potential learning effect and to randomize any influence of the background throughout the scenario.

Participants pressed the horn as quickly as possible when a pedestrian was detected. To signal whether the detected pedestrian was going to collide with the participants or not, they were instructed to press the horn once more to indicate a potential collision or twice more to indicate non-collision. The horn presses allowed us to collect pedestrian detection rate, response time, and collision judgment data.

Data Analysis

A pedestrian was coded as detected if a horn press was recorded after the appearance of the pedestrian. Response time was recorded as the time between pedestrian appearance and the participant's first horn press. Missed pedestrians (i.e., no response) were excluded from the response time analysis. Pedestrians were classified according to whether they appeared in the blind field or the seeing field and the initial bearing angle (80° and 65° in the blind field, 45° in the seeing nasal field, and 45°, 65°, and 80° in the seeing temporal field). Because there was no difference between viewing conditions on the temporal seeing field, we only report data for pedestrians that initially appeared in the blind field (80° and 65°) and the nasal seeing field (45°). The average detection rate and response time of detected pedestrians on all courses were analyzed with a 3 (viewing conditions) × 3 (initial bearing angles) two-way repeated-measures analysis of variance (ANOVA).

Further analyses were conducted with a 3 (viewing conditions) × 3 (initial bearing angles) × 4 (path crossing distances) three-way repeated-measures ANOVA to see the impact of path crossing distance on the detection rate, response time, and collision judgment. We used a linear mixed model in the analyses of response time and collision judgment to account for the number of pedestrians that were not detected.

We used the Greenhouse-Geisser correction to correct the number of degrees of freedom in F distribution. Bonferroni corrected post hoc tests were performed for multiple comparisons of the mean difference. All statistical analyses were performed with SPSS Statistics 24 (IBM, Armonk, NY).

Table. Individual Parameters and Field Expansion Provided by the MxP

ID	Age (y)	Nasal Extent Without Prism (°)	Nasal Extent With Prism (°)	Field Expansion (°)	Theoretical Tilt Angle[13] (°)	Empirical Tilt Angle (°)	Back Vertex Distance (mm)	Monocular Pupillary Distance (mm)
S1	23	50	80	30	7	11	6	35
S2	25	52	81	29	9	10	16	33
S3	24	55	80	25	12	15	11	30
S4	27	60	80	20	14	15	11	29.5
S5	32	60	87	27	16	15	9.5	32.5
S6	24	60	80	20	17	10	10	32
S7	23	58	82	24	10	8	15	32
S8	35	52	80	28	11	9	12	32
S9	28	62	81	19	18	17	9.5	31.5
S10	37	52	80	28	11	13	12	28
R1	21	60	85	25	16	10	17	32.5
R2	70	47	68	21	4	4	12	32.5
R3	41	50	80	30	10	7	12	31.5
AVG	31.5	55.2	80.3	25.1	11.9	11.1	11.8	31.7
SD	12.6	4.8	4.1	3.8	4.0	3.6	2.8	1.7

S, simulated AMV; R, patients with AMV

Results

Visual Field Expansion With MxP Glasses

The Table shows the nasal field extent with and without MxP measured for each subject, as well as the theoretical tilt angles calculated using the monocular pupillary distance and back vertex distance[13] and the empirical tilt angles determined via perimetry.

The average nasal extent of the visual field of participants with simulated AMV was 56.1° ± 4.2° (standard deviation). The MxP glasses configured for each participant provided an average of 25° ± 3.9° of expansion, resulting in an average nasal extent of 81.1° ± 2.1°. In patients with AMV, an average of 25.3° ± 3.7° of expansion was achieved by the MxP glasses. The tilt angle required to obtain the maximum field expansion varied by subject (4°–17°).

Average Pedestrian Detection Rate

The average pedestrian detection rates in each viewing condition and initial bearing angle by participants with simulated AMV are shown in Figure 8A (including all pedestrians on center-to-center collision, near-collision, and non-collision courses). The analyses showed significant main effects of the viewing condition, $F(1.99, 17.93) = 74.15$; $P < 0.01$, and initial bearing angle, $F(1.34,12.1) = 101.71$, $P < 0.01$. There was a significant interaction between the viewing condition and the initial bearing angle for the average pedestrian detection rate, $F(2.62, 23.57) = 29.53$, $P < 0.01$.

For pedestrians initially appearing at 65°, the detection rate in AMV+MxP (95%) was significantly higher than AMV (61%; $P < 0.01$), and there was no significant difference from NV (100%; $P = 0.31$). For pedestrians that initially appeared at 80°, the detection rate in AMV+MxP (61%) was not significantly higher than AMV (50%; $P = 0.2$), but there was a significant difference with NV (98%; $P < 0.01$). The detection rate of the 45° pedestrians on the nasal seeing field remained approximately the same across all viewing conditions (NV, 100%; simulated AMV, 96%; AMV+MxP, 100%; $P > 0.99$), showing that the field expansion via monocular visual confusion and the consequent reduction of contrast did not affect detection performance in the see-through view. There was no difference in detection rate across all viewing conditions on the temporal seeing side (not included in Fig. 8A).

Patients with AMV showed similar performance on the pedestrian detection task compared with the simulated AMV (Fig. 8B). With the MxP glasses, the detection rate of 65° pedestrians improved to 100%

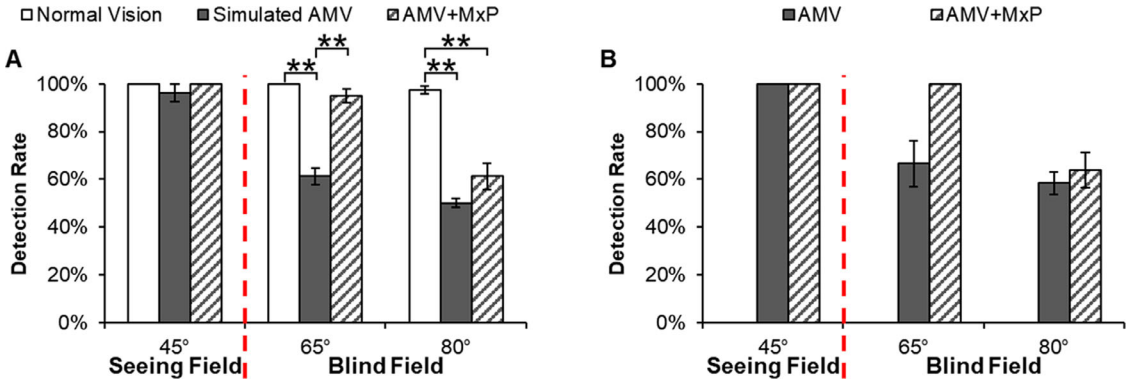

Figure 8. Detection rate of pedestrians with and without MxP glasses. (A) Average detection rate with normal vision, simulated AMV, and AMV+MxP. MxP improved the detection rate in the blind field (65° and 80°) and did not significantly affect the detection rate of the 45° pedestrians. $^{**}P < 0.01$. (B) Average detection rates of the three patients with AMV in both viewing conditions. Statistical analyses were not applied for the three patients with AMV. Error bars are standard errors.

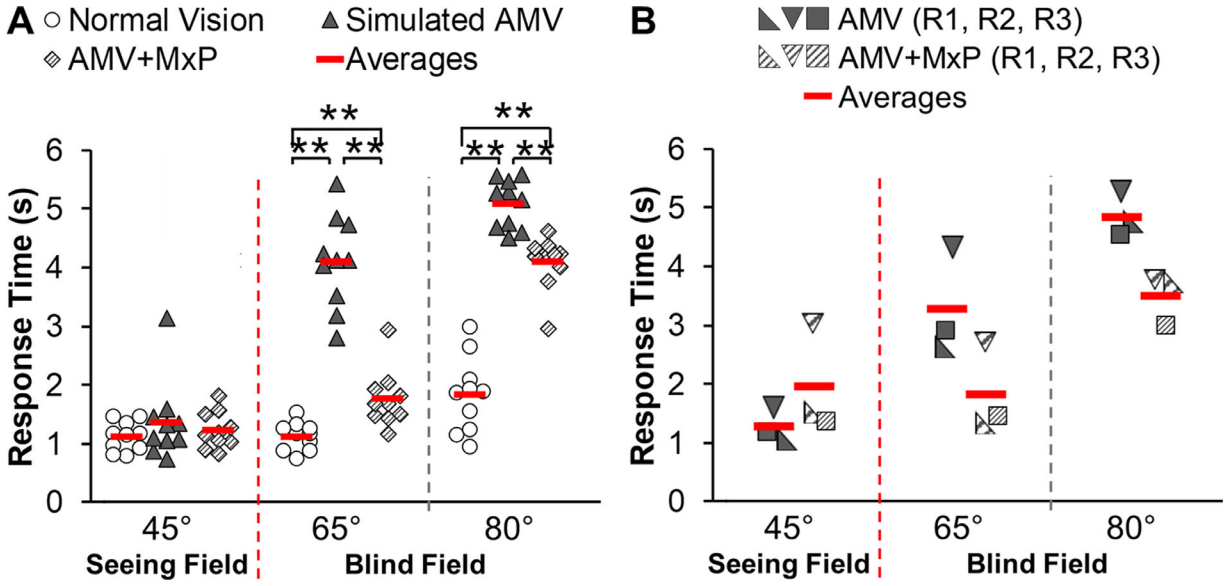

Figure 9. Pedestrian response times with and without MxP glasses. (A) Response times for individual participants with normal vision, simulated AMV, and AMV+MxP. In the blind field, participants responded significantly faster in AMV+MxP than AMV to pedestrians appearing at 65° and 80°. Response times to the 45° pedestrians on the seeing nasal field were not different across conditions. $^{**}P < 0.01$. (B) Response times of the three patients (R1, R2, and R3) with AMV and AMV+MxP. Statistical analyses were not applied for the 3 patients with AMV.

(from 67% without MxP). The detection rate of 80° pedestrians improved to 64% (from 58% without MxP). The detection rate of the 45° pedestrians on the nasal seeing field was 100% under both viewing conditions.

Average Response Time

Because the detection rate was at least 50% in all conditions with simulated AMV, the average response times were representative of detection performance (Fig. 9A). Response times were calculated only for pedestrians that were detected. The analyses showed significant main effects of viewing condition, $F(1.52, 13.7) = 97.41$; $P < 0.01$, and the initial bearing angle, $F(1.89, 16.97) = 296.37$; $P < 0.01$. There was a significant interaction between viewing condition and the initial bearing angle for the average response time, $F(2.49, 22.41) = 71.22$; $P < 0.01$.

Response times for the 65° pedestrians were significantly faster in AMV+MxP (1.8 seconds) than in AMV (4.1 seconds); $P < 0.01$. For the 80° pedestrians, response times were also significantly faster in AMV+MxP (4.1 seconds) than AMV (5.1 seconds); $P < 0.01$. However, the response times in AMV+MxP

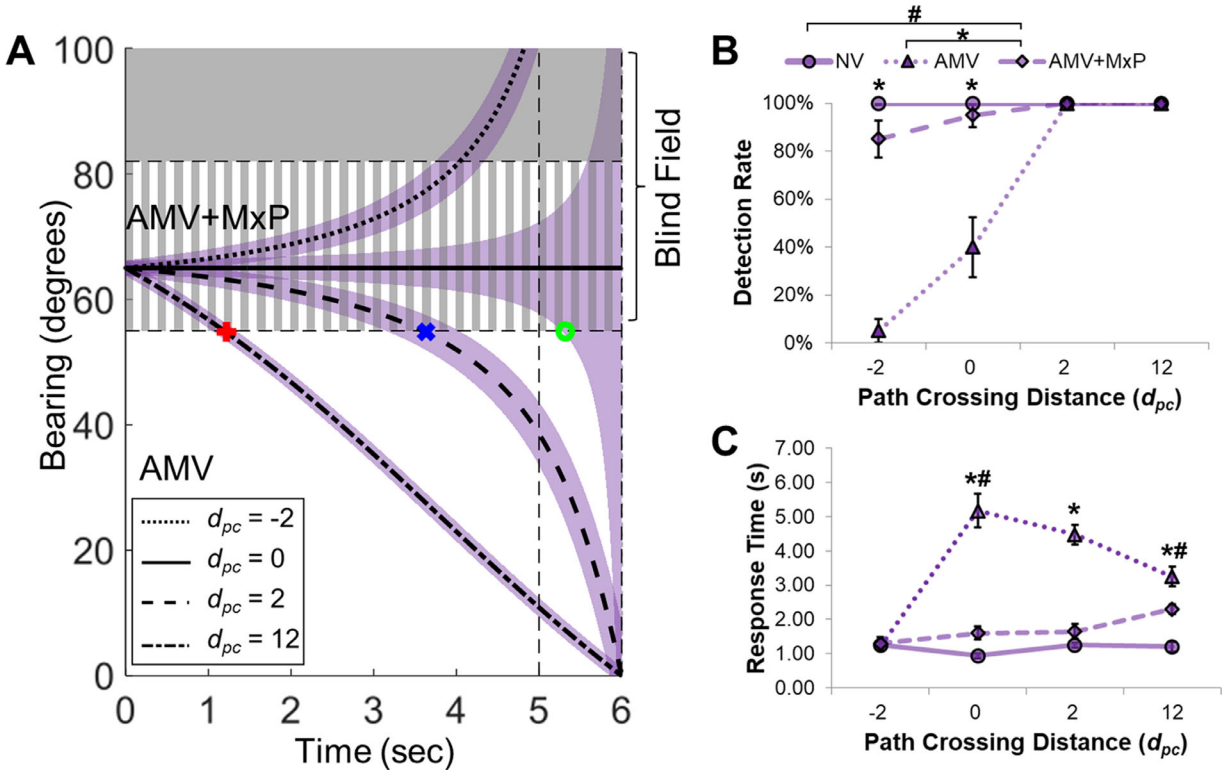

Figure 10. Detection rate and response time for pedestrians initially appearing at a 65° bearing angle with different courses across the viewing conditions. (A) Bearing span as a function of time for pedestrians initially appearing at 65° and walking on four different courses. When the patient is looking straight, the bearing angle of the pedestrian is the same as visual eccentricity. The vertical width in the colored shaded area indicates the horizontal angular size of the pedestrian throughout the event. Colored symbol markers indicate when the pedestrians on different courses enter the seeing field of AMV (red plus, blue cross, and green circle for $d_{pc} = +12$ m, +2 m, and 0, respectively). All pedestrians were visible upon their initial appearance in the AMV+MxP condition (marked with grey vertical gratings). (B) Detection rate and (C) response time to the 65° pedestrians across viewing conditions. In the center-to-center collision course ($d_{pc} = 0$), delayed entering of the pedestrian into the seeing field in AMV resulted in longer response times and lower detection rate. Pedestrians that crossed behind the participant ($d_{pc} = -2$ m) did not enter the seeing field of AMV. In AMV+MxP, the detection rate and response time for pedestrians on all courses were improved. Error bars are standard errors. *, $^{\#}P < 0.01$ for AMV+MxP vs. AMV and AMV+MxP vs. NV, respectively.

were still significantly slower than NV for both 65° pedestrians (1.1 seconds; $P = 0.03$) and 80° pedestrians (1.8 seconds; $P < 0.01$).

There was no significant difference in response times for the 45° pedestrians on the seeing nasal field across all viewing conditions (NV, 1.1 seconds; simulated AMV, 1.4 seconds; AMV+MxP, 1.2 seconds; all Ps > 0.62), which also showed that the monocular visual confusion and the consequent lower contrast did not affect the response time in the see-through view. There was no difference in response times across all viewing conditions on the seeing temporal field (data not shown).

Patients with AMV showed similar improvements in response times with the MxP (Fig. 9B). With the MxP glasses, the response time for 65° pedestrians was improved to 1.8 seconds (from 3.3 seconds without MxP) and for 80° pedestrians was improved to 3.5 seconds (from 4.9 seconds without MxP). Response times for the 45° pedestrians in the seeing nasal field was 1.3 seconds without MxP and 2 seconds with MxP.

Detection Performance With Different Pedestrian Courses

The pedestrian detection performance for each condition was further evaluated for different pedestrian courses (path crossing distance). Except for the center-to-center collision conditions ($d_{pc} = 0$), the bearing angle of approaching pedestrians changed over time (Figs. 10A–12A, see also Supplementary Material, Appendix B2). The bearing angles of pedestrians that would cross in front of the participant ($d_{pc} = +2$ m or +12 m) decrease throughout the event (moving toward the center), while the bearing angles of pedestrians that would cross behind the participant ($d_{pc} = -2$ m) increase over time (moving farther into the periph-

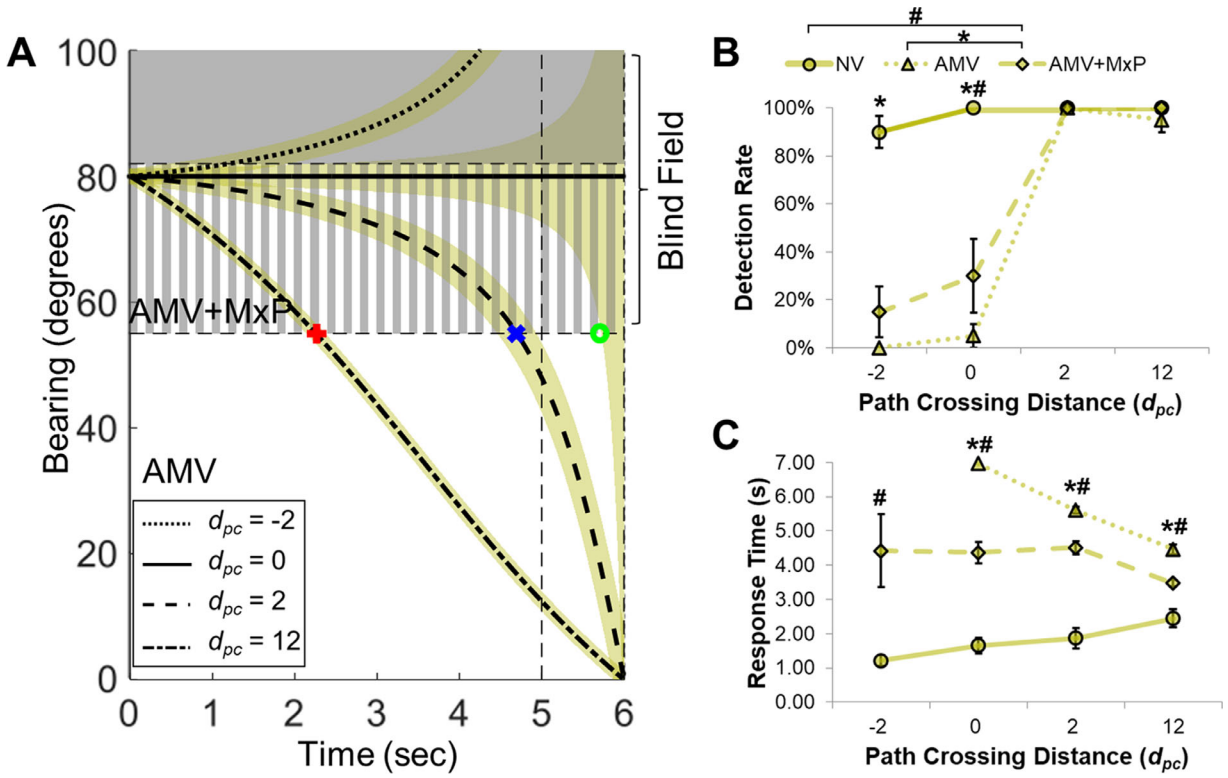

Figure 11. Detection rate and response time for pedestrians initially appearing at 80° bearing with different courses across viewing conditions. (A) Bearing spans as a function of time of 80° pedestrians on different courses. Colored symbols indicate when the pedestrians entered the seeing field of AMV (red plus, blue cross, and green circle for $d_{pc} = +12$ m, +2 m, and 0, respectively). (B) Detection rate and (C) response time of different pedestrian types across viewing conditions. The late entry of the pedestrian into the seeing field resulted in slower response times and reduced detection rates of center-to-center collisions. Pedestrians that passed behind ($d_{pc} = -2$ m) did not appear in the seeing field of AMV. In AMV+MxP, the detection rates and response times of pedestrians on all courses were improved. Error bars are standard errors. *, # $P < 0.01$ for AMV+MxP vs. AMV and AMV+MxP vs. NV, respectively.

ery). The bearing angle changes affected the detection rates (Figs. 10B, 11B, and 12B) and response times (Figs. 10C, 11C, and 12C) due to the appearance timing and duration differences in the pedestrian courses.

There were significant main effects of viewing condition, initial bearing angle, and path crossing distance on detection rate (all Fs > 74.15; all *P*s < 0.01) and response time (all Fs > 12.5; all *P*s < 0.01). The analyses showed a significant three-way interaction for detection rate, $F(3.71, 33.38) = 14.57$; $P < 0.01$, and response time, $F(11, 302.48) = 8.93$; $P < 0.01$. Because there was no detection of 80° pedestrians with $d_{pc} = -2$ m in the AMV condition, this condition was excluded from the response time analysis.

For 65° pedestrians, there was a statistically significant simple two-way interaction between viewing conditions and path crossing distances for detection rates, $F(1.9, 17.07) = 30.03$; $P < 0.01$, and response time, $F(6, 97.55) = 15.59$; $P < 0.01$. The 65° pedestrians in the blind field (Fig. 10) were not visible at an initial appearance with AMV without scanning, while they could be detected in AMV+MxP (Fig. 10A). Pedestrians with an initial bearing angle of 65° and $d_{pc} = -2$ m appeared in the blind field and then moved farther into the periphery, resulting in a detection rate of only 5% with AMV. Pedestrians on center-to-center collision courses ($d_{pc} = 0$) entered the seeing field of AMV at the last moment (5.3 seconds after the initial appearance, green circle in Fig. 10A), and thus the detection rate was significantly decreased (40%) with delayed response time (5.4 seconds) in AMV (all *P*s < 0.01). For 65° pedestrians with $d_{pc} = +2$ m, and +12 m, the pedestrians moved centrally into the seeing field of AMV and thus were detected across all viewing conditions. However, owing to the delayed entering into the seeing field (3.6 seconds in $d_{pc} = +2$ m, blue cross in Fig. 10A; 1.2 seconds in $d_{pc} = +12$ m, red plus in Fig. 10A), the response times were significantly slower with simulated AMV (4.5 seconds in $d_{pc} = +2$ m and 3.2 seconds in $d_{pc} = +12$ m) compared with NV (all *P*s < 0.01).

The detection rates of the 65° pedestrians with $d_{pc} = -2$ m and 0 were significantly improved in AMV+MxP (all *P*s < 0.01) compared with AMV. There was no difference in the detection rate of 65° pedestrians

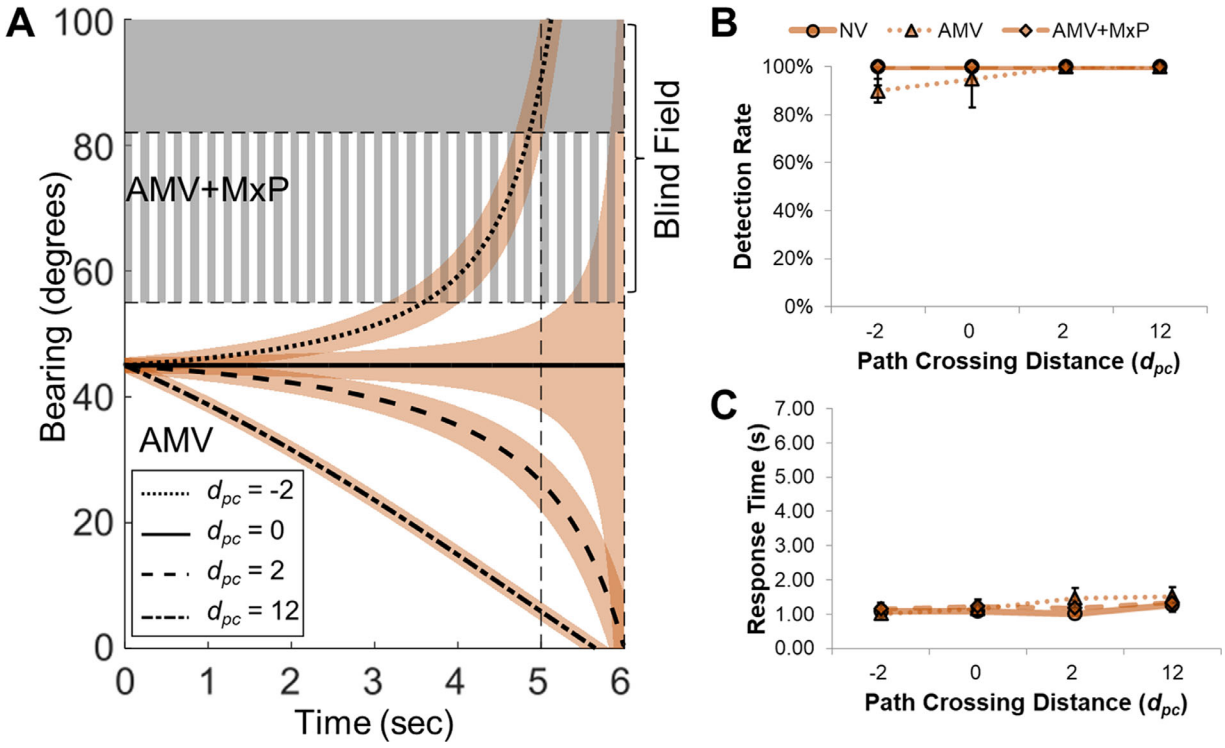

Figure 12. Detection rate and response time for pedestrians that initially appeared at 45° bearing with different courses across viewing conditions. (A) Bearing span of 45° pedestrians on different courses as a function of time. (B) Detection rate and (C) response time of 45° pedestrians on different courses across the viewing conditions. There was no difference in pedestrian detection performance across viewing conditions and courses, which suggests that the MxP did not negatively affect the detection of pedestrians in the see-through view. Error bars are standard errors.

between AMV+MxP and NV for all path crossing distances (all *P*s > 0.24). Response times to the 65° pedestrians for all path crossing distances were significantly better in AMV+MxP compared with AMV (all *P*s < 0.01). However, there was a significant difference in response times to 65° pedestrians between AMV+MxP and NV when the $d_{pc} = 0$ and $d_{pc} = +12$ m (*P*s < 0.01).

The detection rate and response time results for the 80° pedestrians in the blind field of AMV (Fig. 11) were worse than the results with the 65° pedestrians. With the 80° pedestrians, there was a statistically significant simple two-way interaction between viewing condition and path crossing distance for detection rate, $F(2.39, 21.49) = 28.39$; $P < 0.01$, and response time, $F(5, 77.36) = 9.86$; $P < 0.01$. There was no detection of pedestrians with $d_{pc} = -2$ m across all subjects in AMV, and thus this condition was excluded from the response time analysis.

The 80° pedestrians with $d_{pc} = -2$ m were not detected at all in AMV and only 15% were detected in AMV+MxP due to the initial appearance in the blind field (at the edge of the expanded field in AMV+MxP) and continued movement farther into the blind field (exiting the expanded field). Pedestrians on center-to-center collision courses ($d_{pc} = 0$) entered the seeing field of AMV at the very last moment (calculated to be 5.7 seconds after the appearance, green circle in Fig. 11A), and thus the detection rate was very low (5%) with long response times (6.5 seconds in Fig. 11C). The MxP increased the overall detection rate to 30%, but that difference was not statistically significant ($P = 0.29$). The response time was significantly improved to 4.4 seconds ($P < 0.01$). However, both the detection rate and response time for center-to-center collision pedestrians were still significantly worse with AMV+MxP than with NV ($P < 0.01$).

For the 80° pedestrians with $d_{pc} = +2$ m and $d_{pc} = +12$ m, the pedestrians moved into the seeing field of AMV, and thus there was no significant difference in detection rate across viewing conditions. However, pedestrians with $d_{pc} = +2$ m entered the seeing field of AMV 4.7 seconds after initial appearance (blue cross in Fig. 11A) and 2.3 seconds after initial appearance for pedestrians with $d_{pc} = +12$ m (red plus in Fig. 11A) the response times were significantly slower in AMV (5.6 seconds for $d_{pc} = +2$ m and 4.4 seconds for $d_{pc} = +12$ m

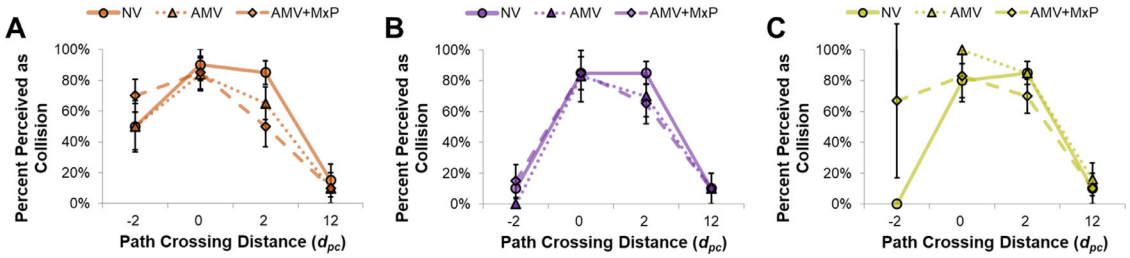

Figure 13. Collision judgment of (A) 45°, (B) 65°, and (C) 80° pedestrians on different courses across viewing conditions. MxP did not significantly affect the collision judgment compared with NV and simulated AMV conditions. Error bars are standard errors.

in Fig. 11C) compared with NV. Response times significantly improved with AMV+MxP (4.5 seconds for d_{pc} = +2 m and 3.5 seconds for d_{pc} = +12 m; all Ps < 0.01), but were still worse than NV (all Ps < 0.01).

Pedestrians in the seeing nasal field that initially appear at 45° are shown in Figure 12. The detection rate and response times of 45° pedestrians were similar across all viewing conditions due to the initial appearance of all pedestrians within the seeing field of AMV (Fig. 12A). There was no statistically significant two-way interaction between viewing condition and path crossing distance for detection rate, F(1, 9) = 1; P = 0.34, or response time, F(6, 109.1) = 0.76; P = 0.61.

Only the average detection rate of the 45° pedestrians with d_{pc} = –2 m in AMV was slightly lower (90%), which may be due to the pedestrian exiting the seeing field of AMV after 3.6 seconds. In AMV+MxP, the average detection rate was the same as NV. Since the 45° pedestrians disappear earlier when d_{pc} = –2 m, there was no delay in the average response time of the detected pedestrians. Because there was no significant difference in the detection rate and response time of 45° pedestrians between NV and AMV+MxP, this finding suggests that the MxP did not impair the detection of pedestrians in the see-through view.

Collision Judgment

To determine the impact of MxP on collision judgment, we used a three-way repeated measure linear mixed model. The analyses found significant main effects of path crossing distance, F(3, 304.58) = 87.53; P < 0.01, and initial bearing angle, F(2, 304. 84) = 3; P = 0.05, but no significant effect of viewing condition, F(2, 304.64) = 0.01; P = 0.99. There was no significant three-way interaction, F(11, 303.28) = 0.25; P = 0.99, but there were significant two-way interactions between viewing condition and path crossing distance, F(6, 303.87) = 2.41; P = 0.03, and between initial bearing angle and path crossing distance, F(6, 303.94) = 2.77; P = 0.01.

For 45° pedestrians in the seeing nasal field (Fig. 13A), there was no significant difference in collision judgment across viewing conditions (all Ps > 0.18), except pedestrians with d_{pc} = +2 m. In AMV+MxP, participants judged 50% of detected near-collision pedestrians that crossed in front of them (d_{pc} = +2 m) as a collision, which is significantly lower than NV (85%; P = 0.01) but not AMV (65%; P = 0.28). Because the 45° pedestrians with d_{pc} = +2 m were in the seeing field for both AMV and NV but had different results, these data are not sufficient to determine whether or not MxP glasses affect collision judgments.

For 65° pedestrians in the blind field (Fig. 13B), collision judgment with AMV+MxP was not significantly different with NV (all Ps > 0.15) or AMV (all Ps > 0.56). For 80° pedestrians in the blind field (Fig. 13C), there was no significant difference in collision judgment among viewing conditions (all Ps > 0.28), except for pedestrians with d_{pc} = –2 m. In AMV+MxP, participants judged 70% of detected pedestrians that crossed behind them (d_{pc} = –2 m) as a collision, which is significantly higher than NV (0%; P = 0.04) but based on a detection rate of only 15%. There was no comparison with AMV because no pedestrians with d_{pc} = –2 m were detected in AMV.

Discussion

Our 3D printed clip-on holder allowed for custom fitting of the MxP segment to provide true field expansion for patients with AMV. We used only two clip-on holders (for left and right simulated AMV) for all 10 simulated AMV participants in the studies to test the fitting generalizability. With an individualized MxP tilt angle (range, 4°–17°), we achieved an average of 25° field expansion for all 13 participants. The clip-on MxP holder was easily customized to ensure proper MxP fit for each subject. However, the current clip-on holder was designed for a specific frame and cannot be fit on other spectacles frames without redesigning the mount-

ing components. The mounting was not designed for daily removal and reattachment by the patients and the tilt adjustment provided may not be practical or desirable in a clinical setting. A universal design of clip-on MxP holder would allow patients to select spectacles frames based on their personal preference and to easily attach and remove it for social and visual needs.

The detection performance for 45° pedestrians in the seeing field with AMV+MxP compared with AMV showed that monocular visual confusion did not significantly affect the performance. Although the average response time in patients with MxP was slightly slower than with simulated AMV, that difference was not significant. The same effect for the patients might have been due to the slow response time of one subject (R2), as shown in Figure 9B. Note that subject R2 had a narrow 48° nasal field and was also the oldest subject.

The MxP significantly improved the detection of the pedestrians in the blind field (65° and 80° pedestrians) compared with AMV. However Yet, the detection performance of the 80° pedestrians in the blind field was significantly worse in AMV+MxP than NV. This could be explained by the strong horizontal minification (more than four times) and lower contrast farthest in the expanded field.[13] The MxP was fit to achieve the highest effective prism power without total internal reflection. Both the shifted and see-through views of the MxP have reduced contrast, a result of the superimposition of two images. We designed the base end of the MxP to have about 25% of the original contrast.[13,16] With this design, the 80° pedestrians were more compressed and had lower contrast than 65° pedestrians in the shifted view. The images of these far pedestrians also fell farther in the periphery where the retinal sensitivity is lower. These might also account for the narrower field expansion (25°) than the theoretical 41° expansion[13] we calculated (Table). The MxP might show a highly compressed and low contrast image of a perimetry target at 41° field expansion, but participants might be unable to detect it due to the minified image of the target falling below detection thresholds. Therefore, the kinetic perimetry target might only be detected at approximately 27° of field expansion where the minified and reduced contrast target exceeded the patient's detection threshold.

One possible improvement might be to introduce an additional 5° of tilt to the MxP to reduce minification and increase contrast.[17] Further tilting of the MxP will provide lower theoretical field expansion but a measured field similar to that calculated. The image quality at the end of the expanded field may be better and thus improve the detection of 80° pedestrians on the side of the blind eye. We plan to further study this fitting option.

Performance on the collision judgment task was consistent with previous results from Qiu et al.,[18] despite very different eccentricities. Although the shifted view presented the pedestrian from the blind field at a different eccentricity in the seeing field, there was no statistically significant difference in collision judgment with the MxP for any of the pedestrian courses (Fig. 13). This finding might indicate that the participants detected the pedestrian first and then made a collision judgment after fixating on the pedestrian. Because of the interference by the prism we did not obtain gaze tracking to confirm this behavior.

Although there was no difference among viewing conditions, the initial bearing angle affected the collision judgment. Qiu et al. (IOVS. 2017;58:ARVO E-Abstract 3287) previously measured collision judgment of pedestrians, approaching from initial bearing angles of 10°, 30°, and 45° with path crossing distances of –4 m, 0, +4 m, and +12 m in the same walking simulator, to determine the near-collision ranges (5 normally sighted subjects). In our study, we measured the collision judgment of pedestrians approaching from 45°, 65°, and 80° initial bearing angles with path crossing distances of –2 m, 0, +2 m, and +12 m. Combining both results, we can estimate how the participants judge collision as a function of initial bearing angles and courses (Fig. 14).

Fewer of the pedestrians that crossed behind the participant (solid symbols) were judged as a collision risk as the eccentricity increased. These pedestrians crossed the participant's path at the same 2 m distance as the near-collision pedestrians that crossed in front (open symbols), yet more of the pedestrians that crossed in front were judged as a collision risk (Fig. 14A).

Figure 14B shows the path crossing distance for 50% collision judgment (50% of detected pedestrians judged as collision) as a function of the initial bearing angle. The pedestrians with closer path crossing distances than the graph in Figure 14B might be perceived as a collision (near collision). Pedestrians that crossed far in front of the participants with a small initial bearing angle (i.e., 8 m at 10° initial bearing angle) were still perceived as a collision, whereas pedestrians that passed more closely behind the participant were not perceived as a collision. With more central initial bearing angles, farther path crossing distances are still perceived as a collision compared to more peripheral initial bearing angles.

Pedestrians that cross behind move farther into the periphery as they walk toward the participant's path, whereas those that cross in front move toward the participant's heading, which may explain the incongruency in collision judgments between the two path types. People may be less concerned with what is happening

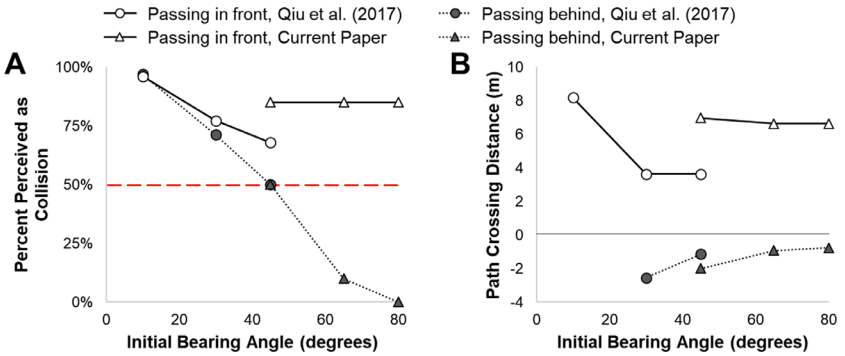

Figure 14. Collision judgment of participants with normal vision for pedestrians approaching on different courses (initial bearing angle and path crossing distance, d_{pc}) based on Qiu et al. (IOVS. 2017;58:ARVO E-Abstract 3287) and the current work. (A) Collision judgment of the pedestrians with the same path crossing distance ($d_{pc} = +2$ m and −2 m) as a function of initial bearing angles. (B) Path crossing distance for 50% collision judgment for pedestrians as a function of initial bearing angles. Pedestrians from more central initial bearing angles that crossed in front of the participant were more often judged as a collision. There is no such effect for those crossing behinds.

behind them because they feel that the social responsibility to avoid a collision is on the other pedestrian, while they may bear responsibility for avoiding potential collisions with a pedestrian that crosses in front of them. We saw similar results in our subjects responses to 45° pedestrians at a path crossing distance of 2m. Participants may judge pedestrians that cross in front of them or with smaller initial bearing angles as more likely to be a collision risk than pedestrians that pass behind or with larger initial bearing angles.

Our current walking simulator scenarios use a simple environment in an open field with the pedestrian as the only nearby object. Patients with AMV complained of bumping into people in crowded environments,[1,3] so continued research should examine how the prism may help with the detection of collision risks in environments with multiple potential hazards surrounding the participant. We tested a low-risk scenario; bumping into another pedestrian is unpleasant event but unlikely to result in severe injury. It would be worthwhile to evaluate the effectiveness of the prisms in higher risk scenarios such as detecting cars at intersections or when approaching a crosswalk.

After a period of adaptation, patients with AMV can drive without restrictions in all jurisdictions. During this period, they are expected to adjust to the loss of binocular depth cues and learn techniques to compensate for the loss of the temporal crescent, such as scanning. They will scan into the blind field when they want to change the lane. However, when a hazard appears in their blind field, they will not know that they need to scan because they cannot see it. The combination of the MxP and the blind spot indicator in the car may be an useful example. Many newer cars have blind spot light indicators on or around the side mirror (about 35° on the driver side and 55° on the passenger side) to alert the driver to approaching vehicles. If the blind eye is on the passenger side, the blind spot indicator is close to the blind field of patients with AMV. The MxP shows the blinking indicator in the blind field in the shifted view. After detection of the lighted alert, AMV drivers can look at the side mirror as normally sighted drivers do.

The MxP may also provide benefits in intersections, which require large scans to check for oncoming vehicles or pedestrians. Drivers with AMV must scan far into the blind field to compensate for the missing temporal crescent. With MxP, AMV drivers may be able to monitor the blind field with smaller head or eye scans and perform large scans only when a hazard is detected through the MxP.

Acknowledgments

Supported by the National Institutes of Health (NIH) grants R01-EY23385 (EP), P30-EY003790 (SERI), and Fight for Sight Grant-in-aid (JJ).

Disclosure: **J.-H. Jung,** None; **R. Castle,** None; **N.M. Kurukuti,** None; **S. Manda,** None; **E. Peli,** (P) (for the multiplexing prisms, assigned to the Schepens Eye Research Institute and licensed to Chadwick Optical, Inc.)

References

1. Coday MP, Warner MA, Jahrling KV, Rubin PA. Acquired monocular vision: functional consequences from the patient's perspective. *Ophthal Plast Reconstr Surg*. 2002;18:56–63.

2. Ihrig C, Schaefer DP. Acquired monocular vision rehabilitation program. *J Rehabil Res Dev*. 2007;44:593–597.
3. Brady FB. *A singular view: the art of seeing with one eye*, 5th ed. Annapolis, MD: Frank B. Brady; 1994.
4. Erie JC, Nevitt MP, Hodge D, Ballard DJ. Incidence of enucleation in a defined population. *Am J Ophthalmol*. 1992;113:138–144.
5. Morgan-Warren PJ, Mehta P, Ahluwalia HS. Visual function and quality of life in patients who had undergone eye removal surgery: a patient survey. *Orbit*. 2013;32:285–293.
6. Kraut JA, Lopez-Fernandez V. Adaptation to monocular vision. *Int Ophthalmol Clin*. 2002;42:203–213.
7. Harrington DO, Drake MV. *The visual fields: text and atlas of clinical perimetry*, 6th ed. St Louis: Mosby; 1990.
8. Good GW, Fogt N, Daum KM, Mitchell GL. Dynamic visual fields of one-eyed observers. *Optometry*. 2005;76:285–292.
9. Peli E, Apfelbaum H, Berson EL, Goldstein RB. The risk of pedestrian collisions with peripheral visual field loss. *J Vis*. 2016;16:1–15.
10. Chardenon A, Montagne G, Buekers MJ, Laurent M. The visual control of ball interception during human locomotion. *Neurosci Lett*. 2002;334:13–16.
11. The National Institute for Rehabilitation Engineering. Vision aids for people having homonymous hemianopsia. 2002. Available at http://www.schepens.harvard.edu/images/stories/nire/one_eye.pdf. Accessed February 5, 2020.
12. The National Institute for Rehabilitation Engineering. Cross-vision glasses for people sighted in one eye. 2002. Available at http://www.schepens.harvard.edu/images/stories/nire/nire_cros_vision_glasses.pdf. Accessed February 5, 2020.
13. Jung J-H, Peli E. Field expansion for acquired monocular vision using a multiplexing prism. *Optom Vis Sci*. 2018;95:814–828.
14. Jung J-H, Peli E. No useful field expansion with full-field prisms. *Optom Vis Sci*. 2018;95:805–813.
15. Apfelbaum HL, Ross NC, Bowers AB, Peli E. Considering apical scotomas, confusion, and diplopia when prescribing prisms for homonymous hemianopia. *Transl Vis Sci Technol*. 2013;2:1–18.
16. Peli E, Jung J-H. Multiplexing prisms for field expansion. *Optom Vis Sci*. 2017;94:817–829.
17. Jung J-H, Peli E. Impact of high power and angle of incidence on prism corrections for visual field loss. *Opt Eng*. 2014;53:P133.
18. Qiu C, Jung J-H, Tuccar-Burak M, Spano L, Goldstein R, Peli E. Measuring pedestrian collision detection with peripheral field loss and the impact of peripheral prisms. *Transl Vis Sci Technol*. 2018;7:1.
19. Deckard CR. University of Texas System, assignee. Method and apparatus for producing parts by selective sintering. United States patent application 920,580 patent 4,863,538, 1989, Sep. 5.
20. Dille JR, Marano JA. The effects of spectacle frames on field of vision. *Aviat Space Environ Med*. 1984;55:957–959.
21. Steel SE, Mackie SW, Walsh G. Visual field defects due to spectacle frames: their prediction and relationship to UK driving standards. *Ophthalmic Physiol Opt*. 1996;16:95–100.
22. Bornstein MH, Bornstein HG. The pace of life. *Nature*. 1976;259:557–559.